Smart Materials and Structures

PAPER

Effect of controlled conductivity on thermal sensing property of 0–3 pyroelectric composite

To cite this article: Gilberto de Campos Fuzari Jr *et al* 2013 *Smart Mater. Struct.* **22** 025015

Smart Mater. Struct. **22** (2013) 025015 (7pp) doi:10.1088/0964-1726/22/2/025015

Effect of controlled conductivity on thermal sensing property of 0–3 pyroelectric composite

Gilberto de Campos Fuzari Jr[1], Marcelo Ornaghi Orlandi[2], Elson Longo[3], Washington Luiz de Barros Melo[4] and Walter Katsumi Sakamoto[5]

[1] Universidade Federal de Mato Grosso—UFMT—Campus do Araguaia, Instituto de Ciências Exatas e da Terra, Barra do Garças (MT), Brazil
[2] Universidade Estadual Paulista—UNESP, Instituto de Química de Araraquara, Araraquara (SP), Brazil
[3] Universidade Federal de São Carlos—UFSCar, Departamento de Química, São Carlos (SP), Brazil
[4] Empresa Brasileira de Pesquisa Agropecuária—EMBRAPA, São Carlos (SP), Brazil
[5] Universidade Estadual Paulista—UNESP, Faculdade de Engenharia de Ilha Solteira, Depto de Física e Química, Avenida Brazil, 56, 15385-000, Ilha Solteira (SP), Brazil

E-mail: sakamoto@dfq.feis.unesp.br

Received 8 August 2012, in final form 4 December 2012
Published 9 January 2013
Online at stacks.iop.org/SMS/22/025015

Abstract
Composite films made of lead zirconate titanate ceramic particles coated with polyaniline and poly(vinylidene fluoride) –PZT-PAni/PVDF were produced by hot pressing the powder mixtures in the desired ceramic volume fraction. The ceramic particles were coated during the polyaniline synthesis and the conductivity of the conductor polymer was controlled by different degrees of protonation. Composites were characterized by Fourier transform infrared spectroscopy (FTIR), scanning electron microscopy (SEM), ac and dc electrical measurements, the longitudinal d_{33} piezo coefficient and the photopyroelectric response. Results showed that the presence of PAni increased the dielectric permittivity of the composite and allowed better efficiency in the poling process, which increased the piezo- and pyroelectric activities of the composite film and reduced both the poling time and the poling electric field. The thermal sensing of the material was also analyzed, showing that this composite can be used as pyroelectric sensor.

1. Introduction

Composites of ferroelectric ceramic filler and polymer matrix (ferroelectric or not) reveal piezo- and pyroelectric activities after a poling process with a suitable electric field. As described by various authors [1–6], these composites are widely used and nowadays are a well-established alternative to conventional ferroelectric materials for actuators, transducers and sensor applications as they combine the electroactive property of the ceramic with the flexibility, formability and mechanical resistance of the polymer.

The easiest and most economical way to fabricate ceramic/polymer composite is by dispersing ceramic particles into the polymer matrix. The obtained composite is termed 0–3, meaning that the dispersion (ceramic particles) is not self-connected in any direction while the polymer phase is self-connected in three directions [7]. This kind of composite has been proposed as a sensor in a wide range of applications [8–13], in spite of the low efficiency of the poling process due to the low dielectric constant of the polymer phase, which decreases the electric field intensity acting on the ceramic particle [14].

To overcome this deficiency many researchers have attempted to improve the poling efficiency by doping the composite with a third semiconductor phase [14–16]. More recently, polyaniline (PAni) has been used to change the electrical conductivity of the composite [17, 18] and several papers have been written about the effect of electrical

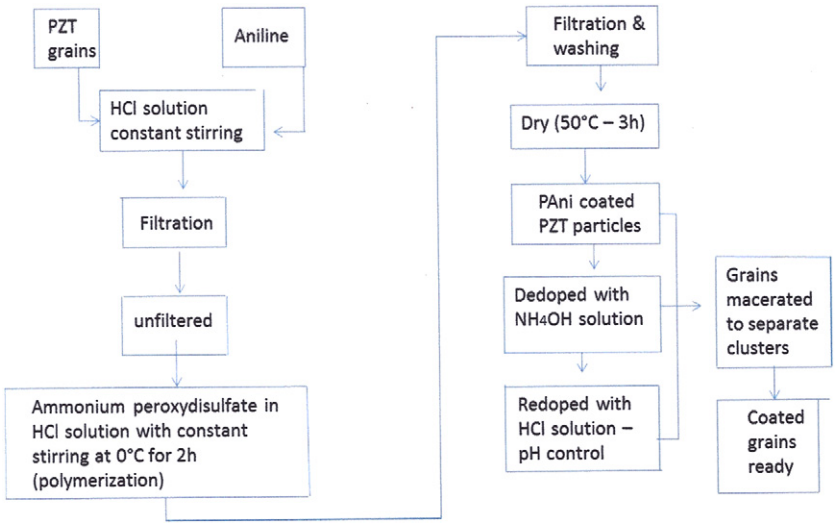

Figure 1. Scheme for PZT-PAni preparation.

conductivity on the electroactive properties of ferroelectric 0–3 composite [19–21].

In this paper we propose a different way to avoid the decrease in the electrical field through a PZT-PAni/PVDF composite film in which PZT particles are coated with PAni instead of adding the PAni as a third phase. The effects of the degree of doping of PAni on the poling process, piezoelectric, pyroelectric and dielectric properties of the composite are discussed. Furthermore, it is shown that the sensing properties of the novel composite film are enhanced when compared with composite films made of PZT particles without the PAni coating. This result is an indication that the material can be used as a pyroelectric sensor.

2. Experimental details

2.1. Synthesis of PAni

Polyaniline was chemically synthesized using ammonium peroxydisulfate $(S_2O_8)^{2-}$ in aqueous 1.0 M of chloride acid (HCl). After filtering and washing, the polyaniline, in powder form, can be dedoped using 0.1 M of ammonium hydroxide treatment [22]. The doping degree of PAni can be modified using a doping solution with different pH values.

2.2. PZT particles coating

PZT particles were incorporated into the solution of aniline and chloride acid and the dispersion was stirred for 1 h and then filtered to release the aniline excess. The block diagram (figure 1) shows all steps of the PZT particles coating.

2.3. Composite preparation

PZT/PVDF and PZT-PAni/PVDF composites were obtained by mixing the ceramic particles with PVDF powder. The mixtures were placed between two Kapton sheets and hot pressed for 1 min at 185 °C, under a constant pressure of 7.6 MPa. The film thickness obtained was in the range between 100 and 300 μm. The volume fraction of ceramic in the composite film was calculated by equation (1) [23]:

$$m_c = \frac{\rho_c}{\rho_p}\frac{\Phi_c}{1-\Phi_c}m_p \tag{1}$$

where m is the mass, ρ is the density and Φ is the volume fraction. The subscripts c and p relate to ceramic and polymer, respectively.

2.4. Measurements

2.4.1. Fourier transform infrared spectroscopy (FTIR). The equipment used in this analysis was a Nexus 670 spectrophotometer (Nicolet) in the range of 2000–4000 cm^{-1}. The measurements were made by diffuse reflectance with a 2 cm^{-1} resolution.

2.4.2. Electron scanning microscopy (FEG-SEM). PZT, PZT-PAni powders and PZT-PAni/PVDF composite film were analyzed by electron microscopy (FEG-SEM—Zeiss model Supra 35) to study the morphology of particles and films.

2.4.3. DC conductivity. PZT, PAni and PZT-PAni tablets were obtained by pressing their powders with a pressure of 11.4 MPa at room temperature. The thickness was about 1 mm and the volumetric conductivity was taken with a Keithley model 236 current source.

2.4.4. Impedance. The impedance measurement was done using an HP 4192A LF analyzer. Data were taken as a function of frequency and stored using a microcontroller device. The dielectric behavior of the sample can also be observed through the impedance spectroscopy since the permittivity (ε) is related to the conductivity (σ) of the sample by [24]:

$$\sigma = \omega\varepsilon'' - i\omega(\varepsilon' - \varepsilon_o) \tag{2}$$

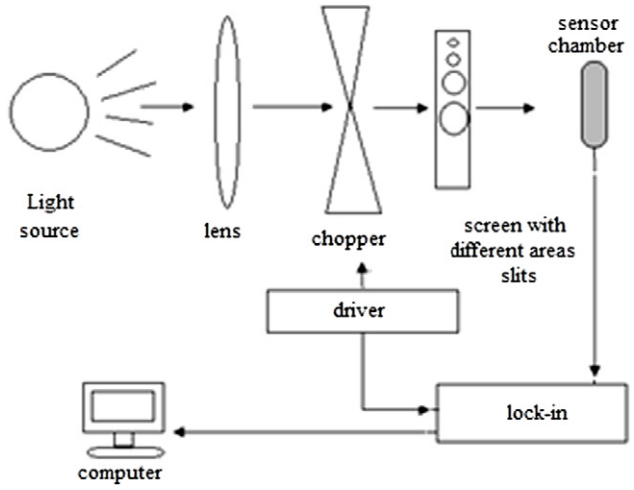

Figure 2. Block diagram of the photopyroelectric detection setup.

where ω is the angular frequency of the external applied electric field, ε_o the vacuum permittivity, and ε' and ε'' are the real and imaginary part of the permittivity, respectively.

2.4.5. Longitudinal d_{33} piezo coefficient. Composite films previously polarized with a Trek model 610 C source in a temperature controlled chamber were analyzed by measuring their piezoelectric activity. The d_{33} piezo coefficient was measured using a Pennebaker model 8000 piezo d_{33} tester (APC) and a 34401A HP multimeter. The poling temperature was 90 °C while the poling time and poling electric field were changed according to the sample requirements.

2.4.6. Pyroelectric activity. The pyroelectric coefficient $p(T)$ was obtained by measuring the pyroelectric reversible current, i.e., measuring the thermally stimulated depolarization current (TSDC) [25] after removing all irreversible contributions to the current, such as injected charge during polarization of the sample. In the direct method [26] of measuring the pyroelectric coefficient, the sample is placed in a temperature controlled chamber with its electrodes shorted and the short-circuit current is monitored. There is no contribution of polarization response due to mechanically clamping or stretching samples, as observed by Li *et al* [27], as in this case the sample is not clamped or stretched.

2.4.7. Photopyroelectric response. The scheme in figure 2 shows the experimental setup to analyze the sensing properties of the pyroelectric material. In the scheme, the sensor is irradiated by a high-power light source (halogen lamp of 250 W) which is chopped to provide modulated radiation. A device assembled in the laboratory is used to change the light intensity sensor, an aluminum strip having openings with diameters ranging from 1 to 10 mm in increments of 1 mm. The sensor element is assembled between two electrodes while it its frontal surface is painted with black ink to maximize the light absorption. The signal from the sensor is measured by a lock-in amplifier model SR530—Stanford Research Systems. The thicknesses of sensor elements are: 180 μm and 220 μm for 30/70 and 50/50 composite samples, respectively.

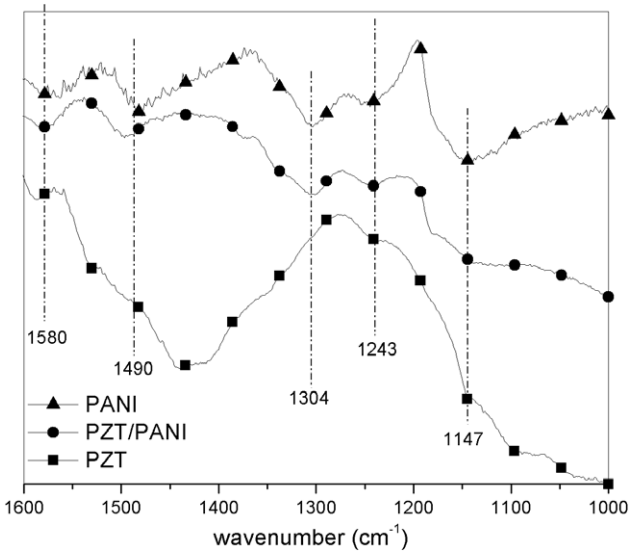

Figure 3. FTIR spectra of PZT, PAni and PZT-PAni particles.

Table 1. Wavenumber/occurrence for PAni [28].

Experimental	Literature	Occurrence
1580	1587	N=Q=N stretching
1490	1495	N–B–N stretching
1304	1303	N–H bending
1243	1259	C–N stretching
1147	1162	B–NH$^+$–B or Q^a = NH$^+$–B
—	829	C–H bending out of plane

3. Results and discussion

To achieve the main objective of this work we need to show that PZT particles were coated by PAni although the green color of particles (characteristic of PAni after protonation) was observed. Figure 3 shows FTIR results for PZT particles, pure PAni and PAni coated PZT particles. Analysis of the FTIR results shows that pure PAni and PZT have completely different spectra. Moreover, it is seen that PZT coated particles have an intermediate spectra presenting some peaks which are characteristic of PAni coverage (peak at 1530 cm^{-1} and broad peak between 1304 and 1490 cm^{-1}). Through these results we can infer that PZT particles were successfully coated by PAni during the synthesis.

Table 1 shows the related peak occurrence with respective wavenumber for PAni. The 1304 cm^{-1} due to the single bond between carbon and nitrogen (C–N) is evidence of PAni, since the PZT curve has no inflexion.

FEG-SEM characterization of pure PZT particles (figure 4(a)) shows that particles are rounded and have sizes between 200 nm and 2 μm. Moreover, it seems that there are many particles aggregated. After the coverage of particles with PAni (figure 4(b)) it is observed that the general morphology is kept but a thin layer of polymer is visible over

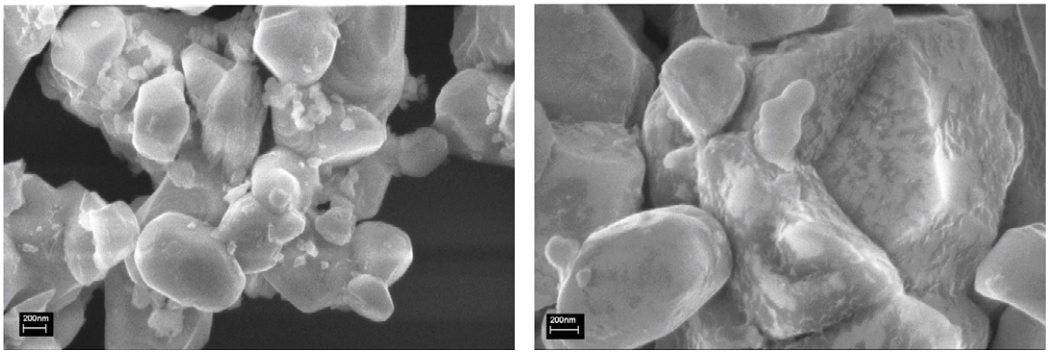

(a) (b)

Figure 4. FEG-SEM image. (a) PZT and (b) PZT-PAni.

Table 2. Electrical resistance of tablets.

Sample	Resistance (Ω)	Method
PZT	604×10^{10}	2-point probe heats
PAni	359×10^{3}	4-point probe heats
PZT-PAni_1	122×10^{6}	4-point probe heats
PZT-PAni_10	137×10^{6}	4-point probe heats

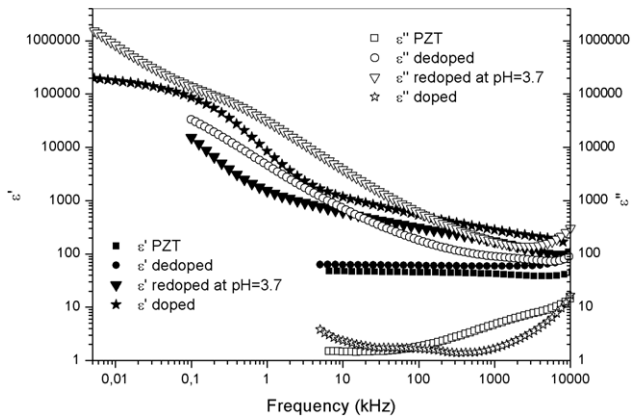

Figure 5. Permittivity of PZT and PZT-PAni particles. All data were acquired at room temperature.

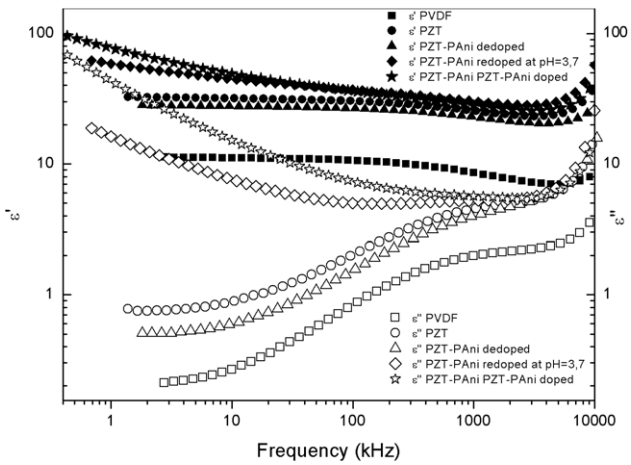

Figure 6. Real and imaginary parts of the permittivity of the composite films. All data were acquired at room temperature.

the whole surface of the particles. It shows that the coating procedure was fully successful and a layer of conductive PAni was deposited on the PZT particles.

The electrical resistance of PZT, PAni and PZT-PAni were also studied. Here, again, results confirm that PAni is covering the PZT particles because the electrical resistance drops by four orders of magnitude as compared with pure PZT. Table 2 shows the electrical measurement results. In PZT-PAni_1 and PZT-PAni_10 samples received 1.0 g and 10.0 g of PZT ceramic powder, respectively.

An important aspect to be observed is the electrical response of the material to an applied alternating electric field. Impedance spectroscopy shows the behavior of dielectric permittivity as a function of frequency. In figure 5 it is clear that there are high values of the permittivity for PZT particles coated with PAni (PZT-PAni) in the low-frequency region. The values of ε' have increased by up to four orders of magnitude for a fully doped PAni coating in comparison with pure PZT. In this case the imaginary part of the permittivity (ε'') is higher than the real part (ε'), indicating high charge mobility, characteristic of the polymer phase (PAni).

Figure 6 shows the behavior of the permittivity of the composite films with 30 vol% of PZT and PZT-PAni. It can be observed that the permittivity values for the composite film with PAni coated PZT particles are higher than for pure PZT. This result confirms the expectation that coating PZT particles with PAni can improve its dielectric constant.

As stated by Wong and Shin [21] the increase of the dielectric permittivity of the polymer matrix in the composite can enhance its piezo- and pyroelectric activities. The point is: the poling field (E) is controlled by the permittivity of the polymer phase because it is much lower than the permittivity of the ceramic. So, for an applied electric field (E_0), the poling field is [15]

$$E = \frac{3\varepsilon_p}{\varepsilon_c + 2\varepsilon_p} E_0 \tag{3}$$

where the subscripts p and c relate to the polymer and ceramic phase, respectively.

From equation (3) is clear that the increase of the dielectric permittivity of the polymer phase (PVDF) can

Table 3. d_{33} coefficient of some composites.

Composite	Volumetric fraction (%)	d_{33} (pC N^{-1})
PSTM/PEKK [34]	50	21
PTCa/PEKK [34]	50	28
PZT/PU + 1% of graphite [35]	49	13
PZT/PVC [16]	30	6
PZT/PVC [16]	50	17
PZT/PVDF with 10% of PAni [17]	50	28
PZT-PAni/PVDF redoped at pH = 3, 7	30	15–20*

Table 4. Pyroelectric coefficient at room temperature [36].

Composite	Volumetric fraction (%)	P (μ C m^{-2} °C^{-1})
PZT/Epoxy	40	40
$BaTiO_3$/rubber	30	60
TGS/PVDF	80	90
PT/PVDF	62	130
PZT/PVDF	50	10
PTCa/P(VDF-TrFE)	65	130
PZT-PAni/PVDF redoped at pH = 3, 7	30	70

make the poling process easier by creating an electrical flux path between the ceramic particles [29, 30]. Dielectric relaxation spectroscopy provides information on the dielectric and electrical behaviors of polymers, and several authors [31, 32] have discussed the increase in the dielectric permittivity as the materials become electrically conductive. The difference in the conductivity in the polymer phase could provide charge separation under an applied electric field and the Maxwell–Wagner–Sillars (MWS) polarization effect could be significant. However, these induced dipoles are not permanent and cannot contribute to the piezoelectric effect.

Wei *et al* [33] have studied the effect of electrical conductivity on the polarization behavior of 0–3 ferroelectric composites and stated that the enhancement of the dielectric permittivity of the polymer phase increases the local electric field acting on the ceramic particle, making the poling process more efficient. In the present paper the same behavior was observed and the higher piezo- and pyroelectric coefficients were attributed to the easier poling process.

The piezo- and pyroelectric coefficients of the PZT-PAni/PVDF composite are displayed in tables 3 and 4, respectively. They are compared with some other ceramic/polymer composites. The longitudinal piezoelectric coefficient (d_{33}) of the composite with 30 vol% of coated PZT is comparable to other composites even with higher ceramic volume fraction (50%). In comparison with PZT/PVC (30 vol%) the value of d_{33} is three times higher.

In table 4 it is shown that the pyroelectric effect of the semiconductor phase (PAni) is also significant. The pyroelectric coefficient $p(T)$ at room temperature is seven times higher than the coefficient of PZT/PVDF (50 vol%) and almost twice that of PZT/epoxy (40 vol%).

So, as the pyroelectric coefficient of this composite is comparable to many other composite in the literature, its ability to convert radiant energy to an electrical signal was analyzed. To be a good photopyroelectric sensor, the relation

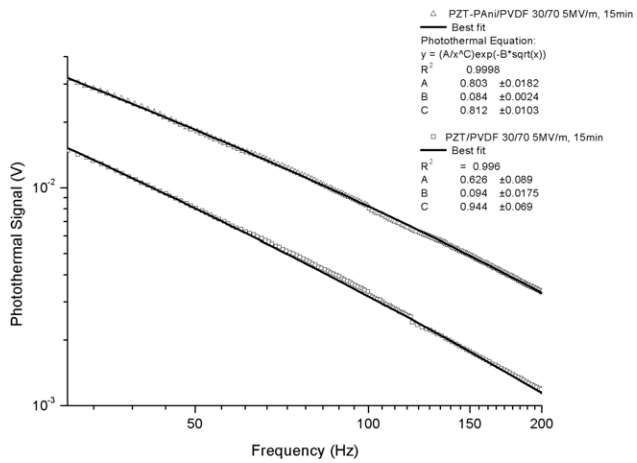

Figure 7. The curve fitting demonstrating the application of equation (4). The solid lines are the better curve fittings.

between the output voltage and the input power must be linear, which means that the responsivity should remain constant. Figure 7 shows the sensor output voltage response as a function of frequency in the range 20–220 Hz. Four samples were used: PZT/PVDF (30/70 vol%) poled with 10 MV m^{-1} for 1 h; PZT/PVDF (50/50 vol%) poled with 10 MV m^{-1} for 1 h; PZT/PVDF (30/70 vol%) poled with 5 MV m^{-1} for 15 min; and PZT-PAni/PVDF (30/70 vol%) poled with 5 MV m^{-1} for 15 min. Higher output signals can be observed for samples of both PZT/PVDF 50/50 vol% poled with a 10 MV m^{-1} electric field for 1 h and for PZT-PAni/PVDF 30/70 vol% poled with a 5 MV m^{-1} electric field for 15 min. Increasing the filler amount increases the output voltage, as we can see for both samples without PAni coating. The advantage of PAni coated composite over the others is the lower time and electric field necessary for the poling process.

The incident light intensity was 0.96 mW for a 1 mm aperture slit. Note that the output voltage behaves as described

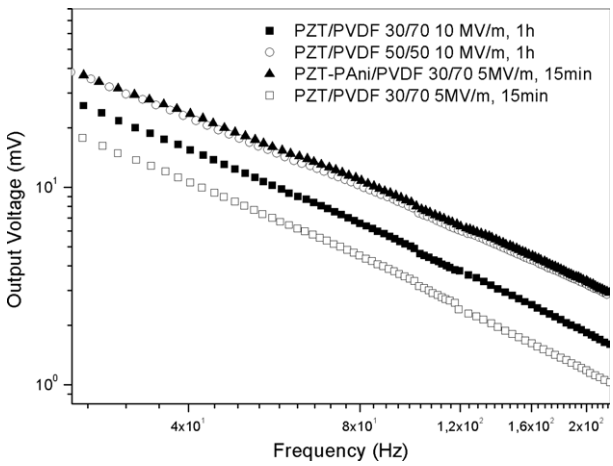

Figure 8. Sensor response to radiant energy.

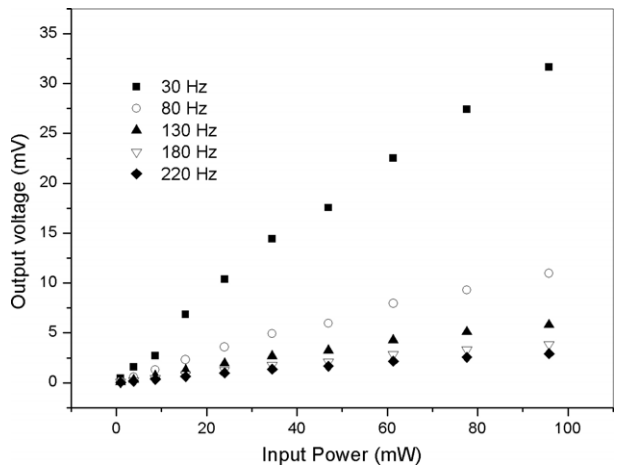

Figure 9. Linear relation between the output signal and input power.

by Mandelis *et al* [37]. The behavior is typical of a thermally thick material, i.e., when the thermal diffusion length is greater than its thickness. The curve fitting using equation (4) shows this behavior giving the fit parameters A, B, C and ω, the amplitude, the modulated frequency exponent, decay exponential coefficient and angular frequency, respectively. The parameter A is a function of the light intensity, the pyroelectric coefficient, dielectric constant etc. The parameter B depends on the thickness (L_s) and the thermal diffusivity of the material (α_s), as $B = \sqrt{\frac{L_s^2}{\alpha_s}}$, and is responsible for the curvature shown in figure 7. The parameter C, may theoretically be 1 or 1.5. In most cases this parameter is unity or close to this, i.e., $C = 1$, as may be seen in figure 7

$$V(\omega) = \frac{A}{\omega^C} \exp[-B\omega^{1/2}]. \tag{4}$$

The legend inside figure 7 shows the parameter values A, B and C. Note that the value C approached unity, as expected for this element sensor. The other parameters indicate the thermal behaviors of these elements, for example, the different values of B depend on the thermal diffusivity of each composite and/or its thickness. While the parameter A shows the electrical response difference between the composite.

Figure 8 shows the behavior of the output voltage for different input powers at several frequencies for the PZT-PAni/PVDF (30/70 vol%) composite. The signal amplitude follows the inverse power law ($1/f$), as expected according to equation (5) [37–39], and the linearity can be observed in the frequency range used.

$$R_v = \frac{V_0}{I_\omega} = \frac{\eta}{cA\omega}\text{FOM} \tag{5}$$

where V_0 is the output voltage, I_ω the input power, η is the absorbed radiant energy fraction, c the specific heat, A the electrode area, ω the frequency and FOM is the pyroelectric figure of merit (p/ε). In figure 9, one can see that the curves slightly diverge from linearity due to the influence of the material thickness and thermal diffusivity, as described by equation (4). If the input power rises then one should expect a tendency for saturation, i.e., a steady signal. So the sensor elements have a good response for a small range of input power and a low modulation frequency.

4. Conclusion

PZT ceramic particles were coated with polyaniline during the synthesis and the composite made of PZT-PAni immersed in PVDF matrix showed a higher dielectric permittivity than composite without the semiconductor phase. This increase in the dielectric constant allowed better efficiency in the poling process. Higher piezo- and pyroelectric coefficients were observed for composites poled with a lower electric field and much lower poling time. Another observed advantage of the semiconductor coating is the lower ceramic volume fraction of the composite film.

PZT-PAni/PVDF composite films have shown the ability to convert radiant energy into electrical signals demonstrating good performance, which indicates that it can be used as a pyroelectric sensor in the low-frequency range to detect low light intensities.

Acknowledgments

Thanks are due to Fundação de Amparo à Pesquisa do Estado de São Paulo—FAPESP and Conselho Nacional de Desenvolvimento Científico e Tecnológico—CNPq, which support the Instituto Nacional de Ciência e Tecnologia de Materiais em Nanotecnologia—INCTMN. W.K.S. also expresses his gratitude to Financiadora de Estudos e Projetos—FINEP through the Rede Interdisciplinar de Nanocompósitos—RIN.

References

[1] Dang Z-M, Fan L-Z, Shen Y and Nan C-W 2003 Study on dielectric behavior of a three-phase CF/(PVDF +$BaTiO_3$) composite *Chem. Phys. Lett.* **369** 95–100

[2] Chew K-H, Shin F G, Ploss B, Chan H L W and Choy C L 2003 Primary and secondary pyroelectric effects of ferroelectric 0–3 composites *J. Appl. Phys.* **94** 1134–45

[3] Zhang D-M, Wei N, Yang F-X, Han X-Y, Zhong Z-C and Zhen K-Y 2006 A new comprehensive model for the pyroelectric property of 0–3 ferroelectric composites *J. Phys. D: Appl. Phys.* **39** 1963–9

[4] Lau S T, Kwok K W, Shin F G and Kopf S 2007 A poling study of lead zirconate titanate/polyurethane 0–3 composites *J. Appl. Phys.* **102** 044104

[5] Das-Gupta D K and Abdullah M J 1988 Electroactive properties of polymer–ceramic composites *Ferroelectrics* **87** 213–38

[6] Furukawa T, Fujino K and Fukada E 1976 Electromechanical properties in the composites of epoxy resin and PZT ceramics *Japan. J. Appl. Phys.* **15** 2119–29

[7] Newnham R E, Skinner D P and Cross L E 1978 Connectivity and piezoelectric-pyroelectric composites *Mater. Res. Bull.* **13** 525–36

[8] Rguiti M, Grondel S, Youbi F E, Coutois C, Lippert M and Leriche A 2006 Optimized piezoelectric sensor for a specific application: detection of Lamb waves *Sensors Actuators* A **126** 362–8

[9] Sun C-L, Lam K H, Wang J, Chan H L W, Zhao X-Z and Choy C L 2006 Precision piezoelectric acoustic position detector *Sensors Actuators* A **128** 290–5

[10] Sakamoto W K, Malmonge J A, Malmonge L F and da Silva A F G 2006 PTCa/PEEK composite acoustic emission sensors *IEEE Trans. Dielectr. Electr. Insul.* **13** 1177–81

[11] Jinhua L, Ningyi Y and Chan H L W 2002 Preparation of PCLT/P(VDF-TrFE) pyroelectric sensor based on plastic film substrate *Sensors Actuators* A **100** 231–5

[12] Sakamoto W K, Higuti R T, de Carvalho A A, Estevam G P, Pontes W and de Paula M H 2009 Piezo and pyroelectric composite film for acoustic emission and x-ray radiation intensity detection *Piezoelectric Materials: Structure, Properties and Applications* ed W G Nelson (New York: Nova Science Publishers) chapter 5, pp 133–47

[13] Sripada S, Unsworth J and Krishnamurty M 1996 PZT/polymer composites for medical ultrasound *Mater. Res. Bull.* **31** 731–9

[14] Sa-Gong G, Safari A, Jang S J and Newnham R E 1986 Poling flexible piezoelectric composites *Ferroelectr. Lett. Sect.* **5** 131–42

[15] Sakamoto W K, de Souza E and Das-Gupta D K 2001 Electroactive properties of flexible piezoelectric composites *Mater. Res.* **4** 201–4

[16] Liu X F, Xiong C X, Sun H-J, Dong L-J, Li R and Liu Y 2006 Piezoelectric and dielectric properties of PZT/PVC and graphite doped with PZT/PVC composites *Mater. Sci. Eng.* B **127** 261–6

[17] Renxin X, Wen C, Jing Z, Yueming L and Huajun S 2006 Dielectric and piezoelectric properties of 0–3 PZT/PVDF composite doped with polyaniline *J. Wuhan Univ. Technol. Mater. Sci. Edn* **21** 84–7

[18] Del Castilho-Castro T, Castilho-Ortega M M and Herrera-Franco P J 2009 Electrical, mechanical and piezo-resistive behavior of a polyaniline/poly(*n*-butyl methacrylate) composite *Composite* A **40** 1573–9

[19] Chau K H, Wong Y W and Shin F G 2007 Enhancement of piezoelectric and pyroelectric properties of composite films using polymer electrolyte matrix *Appl. Phys. Lett.* **91** 252910

[20] Wei N, Zhang D-M, Yang F-X, Han X-Y, Zhong Z-C and Zheng K-Y 2007 Effect of electrical conductivity on the polarization behavior and pyroelectric, piezoelectric property prediction of 0–3 ferroelectric composites *J. Phys. D: Appl. Phys.* **40** 2716–22

[21] Wong C K and Shin F G 2006 Effect of electrical conductivity on poling and the dielectric, pyroelectric and piezoelectric properties of ferroelectric 0–3 composites *J. Mater. Sci.* **41** 229–49

[22] Mattoso L H C and Malmonge L F 1999 Morphology variation as a function of composition for blends of PVDF and a polyaniline derivative *Polymer* **40** 513–8

[23] Marin-Franch P, Martin T, Tunnicliffe D L and Das-Gupta D K 2002 PTCa/PEKK piezo-composites for acoustic emission detection *Sensors Actuators* A **99** 236–43

[24] Clarkson M T 1988 Electrical conductivity and permittivity measurements near the percolation transition in microemulsion. II. Interpretation *Phys. Rev.* A **37** 2079–90

[25] Das-Gupta D K 1991 Pyroelectricity in polymers *Ferroelectrics* **118** 165–89

[26] Byer R L and Roundy C B 1972 Pyroelectric coefficient direct measurement technique and application to a nsec response time detection *Ferroelectrics* **3** 333–8

[27] Li X, Qian X-S, Lu S G, Cheng J, Fang Z and Zhang Q M 2011 Tunable temperature dependence of electrocaloric effect in ferroelectric relaxor poly(vinylidene fluoride-trifluoroethylene-chlorofluoroethylene) terpolymer *Appl. Phys. Lett.* **99** 052907

[28] Tao S, Hong B and Kerong Z 2007 An infrared and Raman spectroscopy study of polyanilines co-doped with metal ions and H^+ *Spectrochim. Acta* A **66** 1364–8

[29] Ploss B and Krause M 2007 Doped polymer as matrix materials for ferroelectric composites *Ferroelectrics* **358** 77–84

[30] Ploss B, Wong Y W and Shin F G 2005 Pyroelectric ceramic/polymer composite with electrically conducting matrix material *Ferroelectrics* **325** 165–9

[31] Lu H, Zhang X and Zhang H 2006 Influence of the relaxation of Maxwell–Wagner–Sillars polarization and dc conductivity on the dielectric behaviors of nylon 1010 *J. Appl. Phys.* **100** 054104

[32] Kanapitsas A and Pissis P 2000 Dielectric relaxation spectroscopy in crosslinked polyurethane based on polymer polyols *Eur. Polym. J.* **36** 1241–50

[33] Wei N, Zhang D-M, Yang F-X, Han X-Y, Zhong Z-C and Zheng K-Y 2007 Effect of electrical conductivity on the polarization behavior and pyroelectric, piezoelectric property of 0–3 ferroelectric composites *J. Phys. D: Appl. Phys.* **40** 2716–22

[34] Peláiz-Barranco A and Marin-Franch P 2005 Piezo-, pyro, ferro- and dielectric properties of ceramic/polymer composites obtained from two modifications of lead titanate *J. Appl. Phys.* **97** 03411

[35] Sakamoto W K, Marin-Franch P and Das-Gupta D K 2002 Characterization and application of PZT/PU and graphite doped PZT/PU composite *Sensors Actuators* A **100** 165–74

[36] Das-Gupta D K 1999 Ferroelectric sensor materials *Mater. Eng.* **10** 97–125

[37] Mandelis A and Zver M M 1985 Theory of photopyroelectric spectroscopy of solids *J. Appl. Phys.* **57** 4421–30

[38] Estevam G P, Melo W L B and Sakamoto W K 2011 Photopyroelectric response of PTCa/PEEK composite *Rev. Sci. Instrum.* **82** 023903

[39] Kao M C, Chen H Z, Yang S L, Chen Y C, Hsieh P T and Yu C C 2008 Pyroelectric Ta-modified $LiNbO_3$ thin films and devices for thermal infrared detection *Thin Solid Films* **516** 5518–22